INTERNATIONAL ATOMIC ENERGY AGENCY
UNITED NATIONS EDUCATIONAL, SCIENTIFIC AND CULTURAL ORGANIZATION
INTERNATIONAL CENTRE FOR THEORETICAL PHYSICS
I.C.T.P., P.O. BOX 586, 34100 TRIESTE, ITALY, CABLE: CENTRATOM TRIESTE

SMR.755/10

Workshop on Fluid Mechanics

(7 - 25 March 1994)

The Atmospheric Boundary Layer
Part I: Mean Vertical Structure

D. Etling
Institut für Meteorologie und Klimatologie
Universität Hannover
Herrenhaüser Str. 2
30149 Hannover
Germany

The Atmospheric Boundary Layer

Part I: Mean Vertical Structure

D. Etling
Institut für Meteorologie und Klimatologie
Universität Hannover, Herrenhäuser Str. 2
30149 Hannover, F.R.G.

Contents

1 Introduction **2**

2 Basic Equations **4**
- 2.1 Averaged Equations 5
- 2.2 First-Order Closure Methods 8

3 The Surface Layer **9**
- 3.1 Turbulent Fluxes 9
- 3.2 Profiles of Mean Variables 11

4 The Ekman Layer **13**
- 4.1 Ekman-Spiral 13
- 4.2 Eddy Viscosity 15
- 4.3 Mixing Length Approach 16
- 4.4 Influence of Thermal Stratification on the Mixing Length 18
- 4.5 Equation for the Turbulent Kinetic Energy 22
- 4.6 Turbulent fluxes 23

5 Applications of ABL theory **26**

6 References **27**

1 Introduction

The **Atmospheric Boundary Layer (ABL)** may be loosely defined as the lowest kilometre of the atmosphere adjacent to the earth's surface. Although only a small part of the whole atmosphere, this boundary layer has a major impact on weather and climate.

This is due to the interactions between the atmosphere and the underlying surface (land or sea) resulting in exchange of energy, momentum, heat, water vapor and air-admixtures. Hence the large scale features in the free atmosphere are predominatly forced by processes originating in the planetary boundary layer.

Unfortunately, processes near the earth's surface are highly inhomogeneous in space and time, yielding a rather complex description of boundary layer phenomena. In order to reduce the vast amount of observational and theoretical knowledge about the real atmospheric boundary layer towards a more concise climatological description, we will focuse on horizontal homogeneous and quasi stationary conditions, i.e., we will restrict ourselves to a description of the mean vertical structure of the ABL.

If the atmospheric motions are treated as a special class of fluid flows one would ask first whether one is dealing with a laminar or a turbulent flow situation. Usually those type of flows are distinguished by the Reynolds number $Re = UD/\nu$, i.e. low Re-number flows (say $Re < 1000$) are termed laminar, and high Re-number flows (say $Re > 10^5$) are called turbulent. Now taking typical values for the lowest part of the atmosphere, the so-called surface layer, we may choose a velocity-scale U = 1 m/s and a vertical height-scale D = 10 m. With the kinematic viscosity of air $\nu = 1.5 \cdot 10^{-5} \mathrm{m}^2/\mathrm{s}$ we get for the surface layer flow $Re \cong 10^6$, hence the atmospheric boundary layer flow is surely turbulent, which has been of course a well accepted fact for long time.

Without starting a lengthly discussion on the question "what is turbulence?" (see books by Tennekes and Lumley (1972), Monin and Yaglom (1975) or Panofsky and Dutton (1984) for more details) we may simply state that in atmospheric boundary layer flows the meteorological variables like wind, temperature and moisture are highly variable in space and time if observed with high spatial and temporal resolution. One example of a high resolution temperature observation is shown in Fig. 1. On the other hand observations of meteorological variables can be very smooth if averaged over space or time, e.g. taking an hourly average for temperature or a 10 minute average for wind velocity. As an example the typical daily variation of the mean temperature near the earth's surface is shown in Fig. 2. More on observations in the turbulent atmospheric boundary layer may be found in books by Oke (1978), Nieuwstadt and van Dop (1982), Lenschow (1986), Arya (1988), Stull (1988) and Garratt (1992).

The Atmospheric Boundary Layer is characterized by strong variations of meteorological variables like wind, temperature and humidity with height. It has become common practice to subdivide the vertical structure of the ABL into three layers. The lowest layer, adjecent to the earth surface, is called viscous sublayer and has a thickness of the order of 1cm. It is assumed that vertical transport of heat, moisture and momentum is due to molecular processes within this thin layer. In meteorological applications this layer is considered seperately only, if exchange processes between the oceans or land surfaces and the atmosphere are treated.

Above the viscous sublayer a region of strong vertical gradients of wind, temperature and humidity can be found, which is called "surface layer". This layer extends up to heights of about 100m above the ground and has been subject of most extensive observational work in the ABL as will be discussed in Chapt. 3.

The third layer, extending up to the top of the ABL, is called "Ekman layer". This may be attributed to the turning of the horizontal wind with height due to action of coriolis forces. The vertical gradients of meteorological variables are usually small compared to those found in the surface layer, hence the Ekman layer is also called "mixed layer" or "well mixed layer" in the literature. The top of the ABL, frequently capped by an temperature inversion aloft, can be observed at a height of 1km or so, but this heigt is subject to strong diurnal variations. Typical profiles for wind and temperature for a daytime ABL can be found in Figure 3.

In the ABL over land the physical processes in the viscous sublayer and in the surface layer are becoming considerable complex if the effect of vegetation has also to be considered. As this would be outside the scope of this lecture, vegetation is treated here only indirectly as surface roughness.

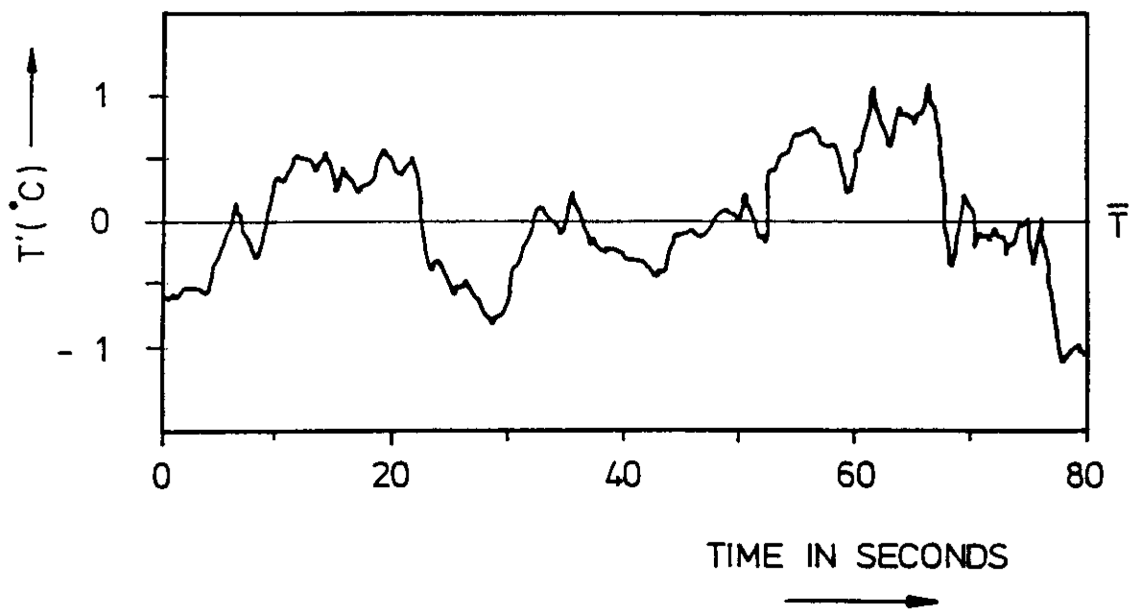

Fig. 1: Short term temporal variations of the temperature fluctuation T'. The mean temperature within the observation period is indicated by $\overline{T}$.

2 Basic Equations

Before we discuss the observed structure of the ABL in some detail, we might derive the underlying physical equations which can be used either for interpretation of the observations of for modelling the atmospheric boundary layer flow.

In any case we need observations for model verification or simply as initial conditions for solving equations. Here we return to the problem of observations in a turbulent flow. As we have seen from Fig. 1 and 2 the variability of the temporal behaviour of atmospheric variables depends strongly on the average over which the measurements are taken. This in turn is related to the problem which one wants to investigate. If one is interested in the turbulence itself one would take high resolution observations (like Fig. 1). But if for practical applications hourly averaged values of e.g. temperature or wind velocity (like Fig. 2) are only needed, filtered observational data are suitable.

For most practical applications of modelling one is interested only in average quantities, like hourly averaged concentration of an air pollutant or ten minute averages of wind speed and wind direction. Hence the models need only solve for averaged variables using also averaged observartions as input. This would not be a problem if atmospheric flows would be laminar and slowly varying. But as we are dealing with a turbulent flow described by nonlinear equations, any averaging proceedure applied to the problem brings the turbulent fluctuations about the mean state back to the model equations, as will be shown below.

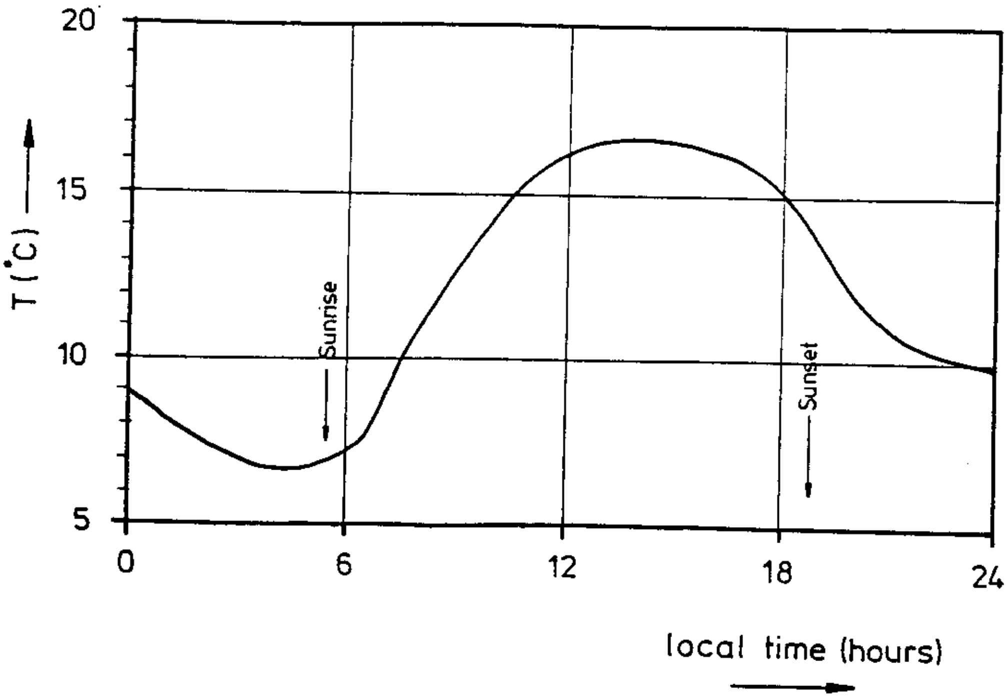

Fig. 2: Typical diurnal variation of air temperature near the ground for spring time in midlatitudes.

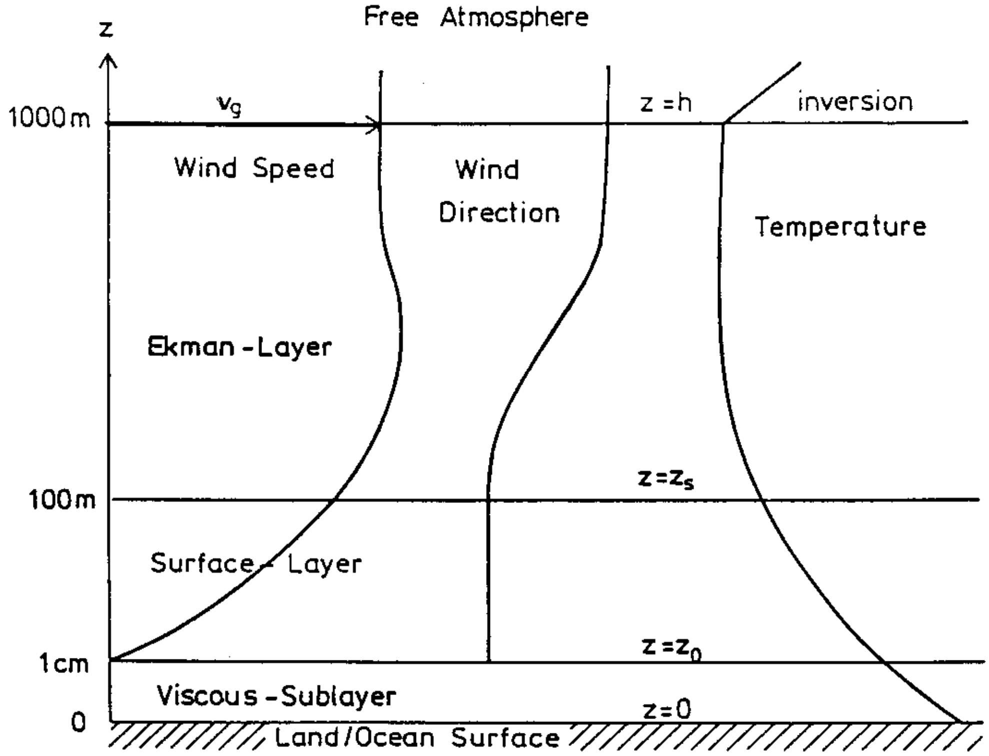

Fig. 3: Typical vertical structure of the daytime atmospheric boundary layer.

2.1 Averaged Equations

In the following we will concentrate on typical equations used in atmospheric modelling for the wind velocity vector u_i, the potential temperature θ and an air-admixture concentration c which could be water vapor or a chemical substance like SO_2, CO etc. We will use the coordinate system as shown in Fig. 4 with velocity components u, v, w in the x, y, z direction respectively (in tensor notation this will be u_1, u_2, u_3 and x_1, x_2, x_3 respectively). In meteorology the vertical coordinate z is directed upwards, the orientation of the horizontal coordinates x and y depends on the problem under investigation. With respect to averaged variables one may take either temporal and spatial averages. Usually locally fixed instruments on towers or on ground stations are taking time averages, moving instruments like on airplanes or integral observing systems from satellites are giving area averages of meteorological variables. A sliding time averaged may be defined by

$$\overline{\phi}(t) = \frac{1}{\Delta t} \int_{-\frac{\Delta t}{2}}^{+\frac{\Delta t}{2}} \phi(t - t')\, dt' \tag{1}$$

Then a variable ϕ can be splitted into an average $\overline{\phi}$ and a deviation ϕ', by:

$$\phi = \overline{\phi} + \phi' \tag{2}$$

with

$$\overline{\phi'} = 0 \tag{3}$$

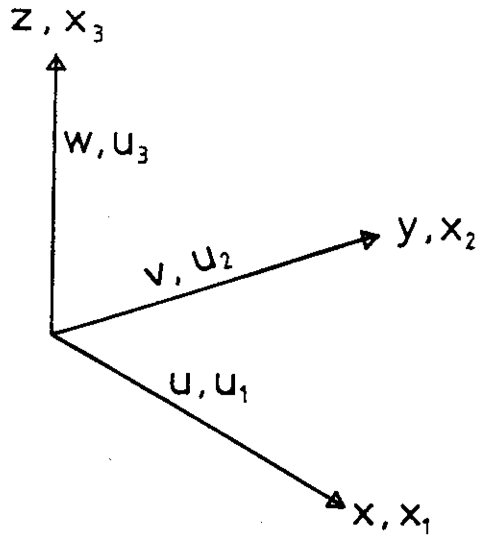

Fig. 4: The co-ordinate system with some notations as used in the text.

by definition of (1).

With respect to numerical modelling or to aircraft measurements one may prefer a spatial average applied to model equations defined by:

$$\hat{\phi}(x,y,z) = \frac{1}{\Delta x \Delta y \Delta z} \int_{-\frac{\Delta x}{2}}^{\frac{\Delta x}{2}} \int_{-\frac{\Delta y}{2}}^{\frac{\Delta y}{2}} \int_{-\frac{\Delta z}{2}}^{\frac{\Delta z}{2}} \phi(x-x', y-y', z-z')\, dx'\, dy'\, dz' \qquad (4)$$

Hence a value $\widehat{\phi}$ represents an average over the gridvolume $\Delta x \Delta y \Delta z$ used in the numerical model.

What kind of average should be applied to atmospheric models is not always obvious as is discussed by Schumann (1975), Deardorff (1973, 1985), Wyngaard (1982), Pielke (1984) or Mellor (1985).

Now as the meteorological equations used for modelling purposes are nonlinear, we have to consider also averages of products like $u_i\phi$. If we split like in (2) $u_i = \overline{u_i} + u_i'$ and $\phi = \overline{\phi} + \phi'$ and apply rules (2) and (3) to the product $u_i\phi$ we obtain:

$$\overline{u_i\phi} = \overline{u_i}\,\overline{\phi} + \overline{u_i'\phi'} \qquad (5)$$

As u_i is the velocity vector we may interpret (5) as a relation for the flux of a quantity ϕ which is splitted (r.h.s. of (5)) into a mean flux of a mean quantity $(\overline{u_i}\,\overline{\phi})$ and so-called "turbulent-flux" $\overline{u_i'\phi'}$. If, for example we take u_i = w and $\phi = \theta$ (potential temperature) we would get $\overline{w\theta} = \overline{w}\,\overline{\theta} + \overline{w'\theta'}$ where $\overline{w'\theta'}$ is usually called "vertical turbulent heat flux" in micrometeorological applications.

At this place we may note, that in atmospheric sciences the so-called potential temperature Θ is frequently used instead of the usual temperature T. Both temperatures are related by

$$\Theta = T\left(\frac{P_0}{P}\right)^{\frac{R}{c_p}} \tag{6}$$

where P_0 is a reference pressure (usually 1000hPa), R is the gas constant for dry air and c_p the specific heat at constant pressure. The potential temperature Θ is thus defined as the temperature an air parcel would attain, if it would be brought adiabatically from its actual pressure p to the reference pressure p_0. Hence Θ is a constant for air parcels for adiabatic processes.

Now the concept of averaging will be applied to the equations describing motions in the atmosphere. The derivations of these equations are not repeated here as they may be found in detail in other texts (see e.g. Businger (1982), Pielke (1984) or Panchev (1985)). The set of equations usually consists of a Boussinesq-approximation of the equation of motions (Eq. 7), the first law of thermodynamics written for the potential temperature $\overline{\theta}$ (Eq. 8) and an equation for the mass-continuity of air-admixtures (Eq. 9) like water vapor or chemical substances. The equations are completed by the continuity equation for incompressible flows (Eq. 10), which is in accordance with the use of the Boussinesq form of (7). The set of equations may be written in standard notation as:

$$\frac{\partial \overline{u_i}}{\partial t} + \overline{u_k}\frac{\partial \overline{u_i}}{\partial x_k} = -\varepsilon_{ijk} f_j \overline{u_k} - \frac{1}{\rho_0}\frac{\partial \overline{p}}{\partial x_i} + g\frac{\overline{\theta} - \theta_0}{\theta_0}\delta_{ik} - \frac{\partial}{\partial x_k}\overline{u_k' u_i'} \tag{7}$$

$$\frac{\partial \overline{\theta}}{\partial t} + \overline{u_i}\frac{\partial \overline{\theta}}{\partial x_i} = S_\theta - \frac{\partial}{\partial x_i}\overline{u_i'\theta'} \tag{8}$$

$$\frac{\partial \overline{c}}{\partial t} + \overline{u_i}\frac{\partial \overline{c}}{\partial x_i} = S_c - \frac{\partial}{\partial x_i}\overline{u_i' c'} \tag{9}$$

$$\frac{\partial \overline{u_i}}{\partial x_i} = 0 \tag{10}$$

In (7) - (10) f is the Coriolis-parameter, ρ_0 and θ_0 are constant reference values for density and temperature and g is gravity. The terms on the r.h.s. of (7) are the coriolis-, pressure- and buoyancy force respectively. The symbols S_θ and S_c denote source and sinks of heat and admixtures respectively. The last terms on the r.h.s. of eq. (7) - (9) are due to the averaging applied to the non-linear advection terms of the unaveraged equations. These terms are called divergence of the Reynolds- stress $\overline{u_k' u_i'}$ (or turbulent friction) in Eq. (7), divergence of the turbulent heat flux $\overline{u_i'\theta'}$ in Eq. 8 and divergence of the turbulent mass flux $\overline{u_i' c'}$ in Eq. (9).

As is evident from (7) - (10) we have four equations for the variables used in atmospheric modelling, i.e. the wind velocity vector $\overline{u_i}$, the potential temperature $\overline{\theta}$, the pressure $\overline{p}$ and the concentration of admixtures $\overline{c}$. But we have as additional unknowns $\overline{u_k' u_i'}, \overline{u_i'\theta'}$, and $\overline{u_i' c'}$, hence the set of equations is not closed. In order to obtain analytical or numerical solutions for these equations one has to close the system, i.e. providing as many equations as variables. This is called the "closure-problem" and is one of the central parts in modelling turbulent flows. Of course this closure problem is not restricted to atmospheric flow phenomena but is inherent also in engineering type of flows. Hence there is a large variety of papers on turbulence and turbulence modelling available in the literature. As examples we mention the textbooks by Monin and Yaglom (1971, 1975), Tennekes and Lumley (1972), Launder and Spalding (1972), Hinze (1975), Bradshaw et al (1981), Panofsky and Dutton (1984), Lesieur (1987) and the review articles by Bodin (1980), Zeman (1981), Wyngaard (1982), Andre (1983), Sommeria (1983), Deardorff (1985), Mellor (1985).

2.2 First-Order Closure Methods

Although many kinds of closure models with different levels of complexity have been proposed (see e.g. Mellor and Yamada, 1974), the most simple method for closing turbulent flow equations (7) - (9) is to relate turbulent fluxes like $\overline{u'_k u'_i}$ or $\overline{u'_i \theta'}$ directly to the mean variables $\overline{u_i}$ or $\overline{\theta}$ by $\overline{u'_k u'_i} = F_1(\overline{u_i}, \overline{\theta}, \overline{c}), \overline{u'_i \theta'} = F_2(\overline{u_i}, \overline{\theta}, \overline{c})$ and $\overline{u'_i c'} = F_3(\overline{u_i}, \overline{\theta}, \overline{c})$, where the functions $F_1 - F_3$ have to be determined. This proceedure is called "parameterization" of turbulent fluxes by first order closure methods. In analogy to diffusion processes in laminar flows it has been become common practice (see e.g. Hinze (1975) or Monin and Yaglom (1975)) to use following special first order closure approximations in turbulence modelling:

Reynolds-stress

$$\overline{u'_k u'_i} = -K_m \left(\frac{\partial \overline{u_i}}{\partial x_k} + \frac{\partial \overline{u_k}}{\partial x_i} \right) + \frac{1}{3} \delta_{ik} \overline{u'^2_i} \qquad (11)$$

where K_m is called "eddy viscosity" or "turbulent diffusion coefficient for momentum" (index: m). In (11) the Reynolds stress is related to the deformation tensor of the mean velocity field (like in Stokes-law for laminar flows). The term $1/3\, \delta_{ik} \overline{u'^2_i}$ on the r.h.s. of (11) (although often neglected) is formally needed for compatibility with the continuity equation (10) if one takes the trace of (11) to yield the turbulent kinetic energy $E = \overline{u'^2_i}/2$.

Turbulent heat flux:

$$\overline{u'_i \theta'} = -K_h \frac{\partial \overline{\theta}}{\partial x_i} \qquad (12)$$

where K_h is called "turbulent diffusion coefficient for heat" (Index: h). Eq. (12) relates the heat flux ($\overline{u'_i \theta'}$ is the kinematic form, $c_p \rho \overline{u'_i \theta'}$ would be the heat flux density in standard units Watt/m^2) to the gradient of the mean temperature $\overline{\theta}$, hence (12) is also called "gradient-transfer relation".

Turbulent mass flux:

$$\overline{u_i'c'} = -K_c \frac{\partial \overline{c}}{\partial x_i} \tag{13}$$

where K_c is called "turbulent diffusivity for admixtures". If, for example, we would take $c = q$ (specific humidity) in (13) K_c would be commonly termed "diffusivity for moisture (K_q) or water vapor (K_w)" in meteorological applications.

Although the closure approximations (11) - (13) have been deducted in analogy to molecular transport processes, the coefficients K_m, K_h and K_c are not material constants of the fluid (air in this case), but are properties of the turbulent flow. Most important, they are not constants like the kinematic viscosity but may vary in space and time, i.e. $K = K(x, y, z, t)$ in general. Hence relations (11) - (13) have closed equations (7) - (9) only to a certain degree, because the coefficients K_m, K_h, K_c have still to be determined. This will be done in more detail in the following chapters.

Another problem disregarded so far is concerned with the anisotropy of the turbulent diffusivities. A more rigorous derivation of first order closure methods (11) - (13) (see textbooks quoted in Chap. 2 for details) would have shown, that the coefficients K_m, K_h and K_c would also depend on the spatial direction of the turbulent fluxes under consideration. Hence $K_x \neq K_y \neq K_z$ (where the index indicates the spatial coordinate) in general as is known from diffusion experiments with airborne materials (see e.g. Pasquill and Smith, 1983). But due to lack of knowledge on the anisotropy of turbulent diffusivities, usually $K_x = K_y = \alpha K_z$ is set in numerical modelling (see e.g. Williams (1972), Sheu et al (1980)), where the range of values for the constant α found in the literature may be given by $1 < \alpha < 100$. On the other hand most numerical schemes used in atmospheric models contain an implicit numerical diffusion, mainly caused by the advection terms, which can exceed the physical horizontal diffusion by an order of magnitude (Pielke, 1984). Hence in the following we will assume the turbulent diffusivities K_m, K_h and K_c, which are also called "exchange coefficients" in the literature, to be isotropic for sake of simplicity.

3 The Surface Layer

3.1 Turbulent Fluxes

Near the earth's surface a shallow layer with strong vertical gradients of wind, temperature and moisture can be observed. This layer, extending up to heights between 10 - 100 m, depending on atmospheric stability is called surface layer (see Fig. 3). There, the wind velocity increases from 0 at the surface to about 70% of it's maximum boundary layer value and the wind direction is nearly constant with height.

As the surface layer is regarded as horizontally homogeneous in the average, only vertical turbulent fluxes are considered in general. Hence the Reynolds stress tensor reduces to the components $\overline{w'u'}$ and $\overline{w'v'}$, the turbulent heat flux to $\overline{w'\theta'}$ and the turbulent mass flux to $\overline{w'c'}$. In the following, the specific humidity q will be taken for c, so $\overline{w'q'}$ may be termed turbulent moisture flux.

In the surface layer, turbulent fluxes are nearly constant with height, which has also led to the terminology "constant-flux-layer". The turbulent fluxes as defined above are usually related to characteristic values for velocity u_*, temperature θ_* and moisture q_* by:

$$u_* = (\overline{w'u'}^2 + \overline{w'v'}^2)^{1/4} \tag{14a}$$

$$\theta_* = -\overline{w'\theta'}/u_* \tag{14b}$$

$$q_* = -\overline{w'q'}/u_* \tag{14c}$$

where u_* is called "friction velocity".

Using (14a - c) a characteristic length can be defined which is a measure of the static stability of the surface layer and is called Monin-Obukhov length L:

$$L = -\frac{u_*^3}{\kappa \frac{g}{\theta} \overline{w'\theta'}} \tag{15}$$

where g is gravity and κ von Kármán's constant.

Since the temperature flux $\overline{w'\theta'}$ in (15) is related to the vertical temperature gradient $\partial\overline{\theta}/\partial z$ by (12), the static stability of the surface layer may be defined by:

$$\frac{1}{L} > 0, \frac{\partial\overline{\theta}}{\partial z} > 0 \quad \text{stable stratification}$$

$$\frac{1}{L} = 0, \frac{\partial\overline{\theta}}{\partial z} = 0 \quad \text{neutral stratification}$$

$$\frac{1}{L} < 0, \frac{\partial\overline{\theta}}{\partial z} < 0 \quad \text{unstable stratification}$$

Since the quantities in (14a - c) and in (15) are independent of height, so called similarity laws, first postulated by Monin and Obukhov (1954), can be set up for the mean vertical profiles of wind speed $\overline{u}$, temperature $\overline{\Theta}$ and moisture $\overline{q}$ in the surface layer. These can be written in dimensionless form:

$$\frac{\kappa z}{u_*}\frac{\partial\overline{u}}{\partial z} = \phi_m\left(\frac{z}{L}\right) , \tag{16a}$$

$$\frac{\kappa z}{\theta_*}\frac{\partial\overline{\theta}}{\partial z} = \phi_h\left(\frac{z}{L}\right) , \tag{16b}$$

$$\frac{\kappa z}{q_*}\frac{\partial\overline{q}}{\partial z} = \phi_w\left(\frac{z}{L}\right) . \tag{16c}$$

The universal functions ϕ_m, ϕ_h and ϕ_w have to be determined from observations. This has been done extensively during the last three decades. Examples can be found among others in papers by Businger et al. (1971), Dyer (1974), Yaglom (1977) or Mc Bean (1979).

Although many observational experiments have been performed, there is no general agreement as to the exact values of the ϕ-functions, most data can be fitted to analytical functions as given by:

(a) unstable stratification (z/L <0):

$$\phi_m = \left(1-\beta_m\frac{z}{L}\right)^{-1/4}, \quad (17a)$$

$$\phi_h = \alpha_h\left(1-\beta_h\frac{z}{L}\right)^{-1/2}, \quad (17b)$$

$$\phi_w = \alpha_w\left(1-\beta_w\frac{z}{L}\right)^{-1/2}. \quad (17c)$$

(b) stable stratification ($z/L > 0$):

$$\phi_m = 1 + \gamma_m\frac{z}{L}, \quad (18a)$$

$$\phi_h = \alpha_h + \gamma_h\frac{z}{L}, \quad (18b)$$

$$\phi_w = \alpha_w + \gamma_w\frac{z}{L}. \quad (18c)$$

For neutral stratification the ϕ-functions can be derived from (17) of (18) by setting $z/L = 0$. As an example of several evaluations of the constants used in (17) and (18) (see Dyer (1974), Yaglom (1977), Etling (1987) for a collection) the widely used data sets by Businger et al (1971) and Dyer (1974) are given below:

Businger et al (1971):

$$\kappa = 0.35,\ \alpha_h = 0.74,\ \beta_m = 15,\ \beta_h = 9,\ \gamma_m = 4.7,\ \gamma_h = 4.7$$

Dyer (1974):

$$\kappa = 0.41,\ \alpha_h = 1,\ \beta_m = 16,\ \beta_h = 16,\ \gamma_m = 5.0,\ \gamma_h = 5.0$$

Profile functions ϕ_w for water vapor are commonly set equal to ϕ_h, as is indicated from the few measurements available (Pruitt et al (1973), Brutsaert (1982)). Thus for ϕ_w one would set $\alpha_w = \alpha_h$, $\beta_w = \beta_h$ and $\gamma_w = \gamma_h$ in (17c) and (18c).

3.2 Profiles of Mean Variables

In atmospheric boundary layer models the flux-gradient relations (16a-c) are often used to obtain the surface fluxes of momentum, heat and moisture from the mean variables at the lowest grid point of the model. In this way the strong vertical gradients in the surface layer need not to be resolved explicit by the model grid. If the lowest grid point is located between $z_0 \leq z \leq z_s$, where z_s is the top of the surface layer, the mean profiles can be obtained by integrating (16a-c) using empirical functions (17a-c) and (18a-c).

In case of neutral stratification ($z/L = 0$) $\phi_m = 1$ and integration of (16a) yields the so called "logarithmic wind profile":

$$\overline{u}(z) = \frac{u_*}{\kappa} \ln \frac{z}{z_0} \quad (z \geq z_0) \tag{19}$$

z_0 is the so called "roughness length", which is defined as the height above ground ($z = 0$) for which the mean wind velocity $\overline{u}$ vanishes, i.e. $\overline{u}(z_0) = 0$. The value of z_0 depends on the surface structure (e.g. $z_0 = 0.1$ cm for bare soil, $z_0 = 5$ cm for grass).

For stable stratification ($z/L > 0$) (16a-c) can be integrated using the general form (18a-c) yielding the so-called "log + linear" profiles of the surface layer:

$$\overline{u}(z) = \frac{u_*}{\kappa}\left(\ln \frac{z}{z_0} + \gamma_m \frac{z}{L}\right) \tag{20a}$$

$$\overline{\theta}(z) = \overline{\theta}(z_0) + \frac{\theta_*}{\kappa}\left(\alpha_h \ln \frac{z}{z_0} + \gamma_h \frac{z}{L}\right) \tag{20b}$$

$$\overline{q}(z) = \overline{q}(z_o) + \frac{q_*}{\kappa}\left(\alpha_w \ln \frac{z}{z_0} + \gamma_w \frac{z}{L}\right) \tag{20c}$$

For unstable stratification ($z/L < 0$), Paulson (1970) obtained an analytic solution for (16a-c):

$$\overline{u}(z) = \frac{u_*}{\kappa}\left(\ln \frac{z}{z_0} - \psi_m\left(\frac{z}{L}\right)\right) \tag{21a}$$

$$\overline{\theta}(z) = \overline{\theta}(z_0) + \alpha_h \frac{\theta_*}{\kappa}\left(\ln \frac{z}{z_0} - \psi_h\left(\frac{z}{L}\right)\right) \tag{21b}$$

$$\overline{q}(z) = \overline{q}(z_0) + \alpha_w \frac{q_*}{\kappa}\left(\ln \frac{z}{z_0} - \phi_w\left(\frac{z}{L}\right)\right) \tag{21c}$$

where the abreviations

$$\begin{aligned}
\psi_m &= 2\ln \frac{(1+x)}{2} + \ln \frac{1+x^2}{2} - 2\tan^{-1} x + \frac{\pi}{2}, \; x = \left(1 - \beta_m \frac{z}{L}\right)^{1/4} \\
\psi_h &= \ln \frac{1+y}{2} \qquad , y = \left(1 - \beta_h \frac{z}{L}\right)^{1/2} \\
\psi_w &= \psi_h
\end{aligned}$$

have been used. Note that $\overline{u}(z)$ in (19) - (21) denotes the magnitude of the wind vector $\overline{u_i}$, since the wind direction does not change with height within the surface layer by definition.

From the similarity laws (16a-c) one can get also informations on the turbulent diffusivities K_m, K_h and K_w in the surface layer. Combining first order closure relations (11), (12), (13) with the similarity laws (16a-c) one obtains

$$K_m(z) = \kappa u_* z \phi_m^{-1} \quad (22a)$$

$$K_h(z) = \kappa u_* z \phi_h^{-1} \quad (22b)$$

$$K_w(z) = \kappa u_* z \phi_w^{-1} \quad (22c)$$

For neutral stratification, K_m increases linearly with height. The eddy diffusivity for water vapor K_w is usually set equal to K_h. The ration K_m/K_h, called "Turbulent Prandtl Number", is derived from (22a,b) as:

$$\frac{K_m}{K_h} = \frac{\phi_h}{\phi_m} \quad (23)$$

For modelling purposes equations (20a-c) may be used for the evaluation of the turbulent fluxes in the surface layer (i.e. $\overline{w'u'}, \overline{w'v'}, \overline{w'\theta'}, \overline{w'q'}$) from the knowledge of the computed values $\overline{u}(z_s), \overline{v}(z_s), \overline{\theta}(z_s), \overline{q}(z_s)$ and the boundary values $\overline{\theta}(z_0), \overline{q}(z_0)$, where z_s is the height of the surface layer, generally the lowest computational grid point of the model, and z_0 is the roughness length. But as the similarity functions (17a-c) and (18a-c) as well as the integral solutions (20a-c), (21a-c) depend on the Monin-Obukhov length L, which in turn contains $\overline{w'\theta'}$ and u_*, this evaluation can be done only by some iterative methods. But as the numerical solution of the model equations (7) - (11) has to be performed by iteration proceedures anyhow, it should be no problem to incorporate surface-layer parameterization described above into atmospheric models (Busch et al, 1976). If e.g. a temporal integration has to be performed one could use the Obukhov- length L form the previous time step (L(t)) for evaluation of e.g. $u_*(t+\Delta t)$ from $\overline{u}(t+\Delta t)$ after (20a) or (21a) without too large error for small time steps (say 60s). But one may also use an explicit method without iteration in the surface layer, which was developed by Louis (1979) especially for application to operational weather forecast models with large time steps (Louis et al, 1981).

4 The Ekman Layer

4.1 Ekman-Spiral

Let us consider on atmospheric boundary which is homogeneous in the horizontal direction except for the pressure forces. If we apply first order closure methods (Eqs. 11, 12) to the equation of motion (7) and the first law of thermodynamics (8), we get following simplified equations:

$$\frac{\partial \overline{u}}{\partial t} - f\overline{v} = -\frac{1}{\overline{\varrho}}\frac{\partial \overline{p}}{\partial x} + \frac{\partial}{\partial z} K_m \frac{\partial \overline{u}}{\partial z} \quad (24a)$$

$$\frac{\partial \overline{v}}{\partial u} + f\overline{u} = -\frac{1}{\varrho}\frac{\partial \overline{p}}{\partial y} + \frac{\partial}{\partial z}K_m\frac{\partial \overline{v}}{\partial z} \tag{24b}$$

$$\frac{\partial \overline{\Theta}}{\partial t} = -\frac{1}{\varrho c_p}\frac{\partial R}{\partial z} + \frac{\partial}{\partial z}K_h\frac{\partial \overline{\Theta}}{\partial z} \tag{24c}$$

In (24c) R represents the net vertical energy flux due to long wave and short wave radiation which we might consider as the only source term S_Θ from (8).

In the following, we will focus only on the equations of motion (24a,b). If we further consider a stationary and frictionless atmospheric flow, we obtain an equilibrium between Coriolis force and pressure force, which can be written in vector notation as:

$$f\vec{k} \times \vec{v} = -\frac{1}{\varrho}\vec{\nabla}\overline{p} \tag{25}$$

where $\vec{k}$ is the vertical unit vector.

The wind velocity $\vec{v}$ fullfilling condition (25) is called "geostrophic wind" and is usually defined by:

$$\vec{v}_g = \frac{1}{\overline{\varrho} f}\vec{k} \times \vec{\nabla}\overline{p} \tag{26}$$

If we now allow frictional forces to be considered, but still for steady conditions, equations (24a,b) can be written with the aid of (26) as:

$$-f(\overline{v} - v_g) = \frac{\partial}{\partial z}K_m\frac{\partial \overline{u}}{\partial z} \tag{27a}$$

$$+f(\overline{u} - u_g) = \frac{\partial}{\partial z}K_m\frac{\partial \overline{v}}{\partial z} \tag{27b}$$

where u_g, v_g are the components of the geostrophic wind defined in (26). Equations (27a,b) are called Ekman-layer-equations and can be solved subject to the prescription on the eddy viscosity K_m. Solutions of these equations for arbitrary profiles $K_m(z)$ will be discussed later. Here we consider the most simple case with $K_m =$ constant. With the boundary conditions

$\overline{u} = \overline{v} = 0 \quad , \quad z = 0$

$\overline{u} = u_g \ , \ \overline{v} = 0 \ , \ z \to \infty$

the classical Ekman solution (Ekman, 1905) is obtained for (27a,b) as:

$$\overline{u}(z) = u_g[1 - e^{-\frac{z}{D}}\cos\left(\frac{z}{D}\right)] \tag{28a}$$

$$\overline{v}(z) = u_g\, e^{-\frac{z}{D}}\sin\frac{z}{D} \tag{28b}$$

In solving (27a,b) the coordinate has been orientated with the x-axis in the direction of the geostrophic wind vector $\vec{v}_g$, hence $v_g = 0$. In (28a,b) D is the so called Ekman length

$$D = (2K_m/f)^{\frac{1}{2}} \tag{29}$$

Solution (28a,b) is shown in Fig. 5 as a hodograph of the horizontal wind vector $\vec{\bar{v}}$, where the $\bar{u}$-component is defined parallel to the direction of the geostrophic wind $\vec{v}_g$. Although highly idealized, solution (28a,b) contains the pronounced feature of the ABL, namely the turning of the wind with height due to the combined action of pressure, coriolis and friction-forces. The angle α between the surface wind (near $z = 0$) and the geostrophic wind is 45° for the analytic solution (28a,b), which is more than the observed values of about 20°. The reason is, that a constant eddy viscosity K_m has been employed which is not quite appropriate for a turbulent boundary layer.

The height of the ABL can also be estimated from (28a,b). If we define this as the height h, where the wind $\vec{v}$ is parallel to the geostrophic wind $\vec{v_g}$ for the first time (i.e. $\bar{v} = 0$) we obtain $h = \pi D$. In the example given in Fig. 5 we get $h \simeq 1000$m, which can be regarded as an typical value for height of the neutrally stratified ABL.

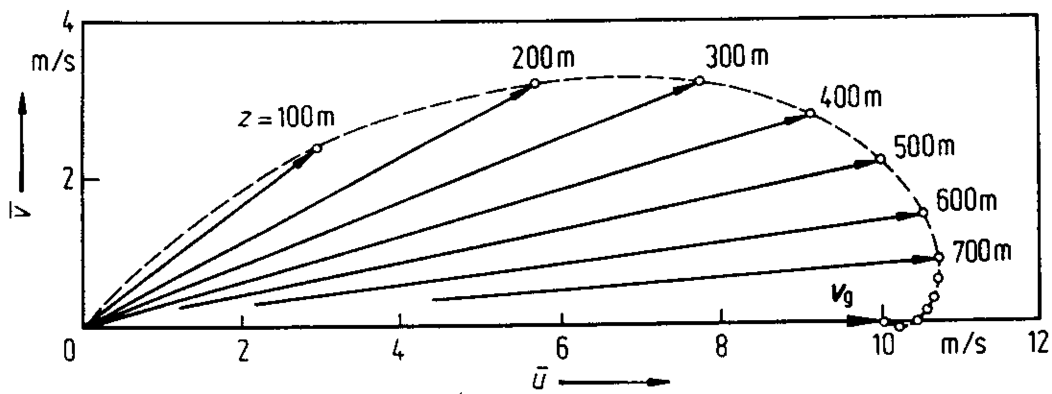

Fig. 5: Hodograph of the horizontal wind after analytical solution (28a,b) (Ekman spiral) for $|\vec{v}_g| = 10\text{ms}^{-1}$, $K_m = 5\text{ms}^{-1}$ and $f = 10^{-4}\ \text{s}^{-1}(\varphi = 43°)$.

4.2 Eddy Viscosity

The so-called Ekman-spiral (Fig. 5) is hardly ever observed in the atmosphere. This is not only because ideal conditions (steady state, horizontally homogeneous situation) are not easy to be found in the real world, but also because the restricting assumption of an eddy viscosity constant with height (K_m = constant) has been used in solving Eqs. (27a,b). In reality, K_m (and also K_h and K_c) are not properties of the fluid but properties of the flow. In fact the eddy viscosity K_m (and K_h, K_c) is dependent on the wind speed and thermal stratification and may therefore vary considerable in space and time. Hence there is only limited use in giving explicit formulations for K_m, K_h and K_c valid for all situations in atmospheric flows.

Although there have been numerous proposals for vertical profiles of eddy diffusivities (see e.q. Wippermann (1973) or Mc Bean (1979) for a collection), we will give only some typical examples. As the values of diffusivities for heat (K_h) are usually directly related to the eddy viscosity K_m, we will concentrate on the latter. Some proposed profiles are:

Neutral stratification (Wippermann, 1973):

$$K_m(z) = \kappa u_* z e^{-7.6(\frac{z}{H})^{0.764}} \tag{30}$$

with $H = \kappa u_*/f$ as the height of the boundary layer.

Stable stratification (Brost and Wyngaard, 1978):

$$K_m(z) = \kappa u_* z \frac{(1 - \frac{z}{h})^{1.5}}{1 + 4.7\frac{z}{L}} \tag{31}$$

where h is the height of the stable boundary layer.

Unstable stratification (Moeng and Wyngaard, 1984):

$$K_m = 2.5 w_* z_i \left(1 - \frac{z}{z_i}\right)\left(\frac{z}{z_i}\right)^{3/2} \tag{32}$$

where z_i is the height of the capping inversion. In (26) w_* denotes the so-called convective velocity scale defined as $w_* = \left(z_i\, g/\theta_0\, \overline{w'\theta'_0}\right)^{1/3}$.

In all empirial functions (30) - (32) the friction velocity u_* and the surface heat flux $\overline{w'\theta'_0}$ as well as the height of the boundary layer has to be known. These parameters can be obtained from other model variables during the computation proceedure or from observations if available.

Although relations (30) - (32) are only examples of several possible functions proposed by different authors, they are based on the typical behaviour of the eddy viscosity in the atmospheric boundary layer: an increase near the surface height, a maximum in the lower part and a decrease in the upper layer. Also the magnitude varies with thermal stratification: small values (say 1m^2/s) for stable, larger values (say 10 m^2/s) for neutral and large values (say 100 m^2/s) for unstable stratification. This qualitative behaviour is illustrated in Fig. 6.

4.3 Mixing Length Approach

As stated before, the turbulent diffusivities K_m, K_h and K_c are usually not fixed in time and space as is suggested by empirical formulae like (30) - (32), but are properties of the flow, which might be quite complex in certain atmospheric situations. In order to take the variability of diffusion coefficients into account the so-called "mixing-length

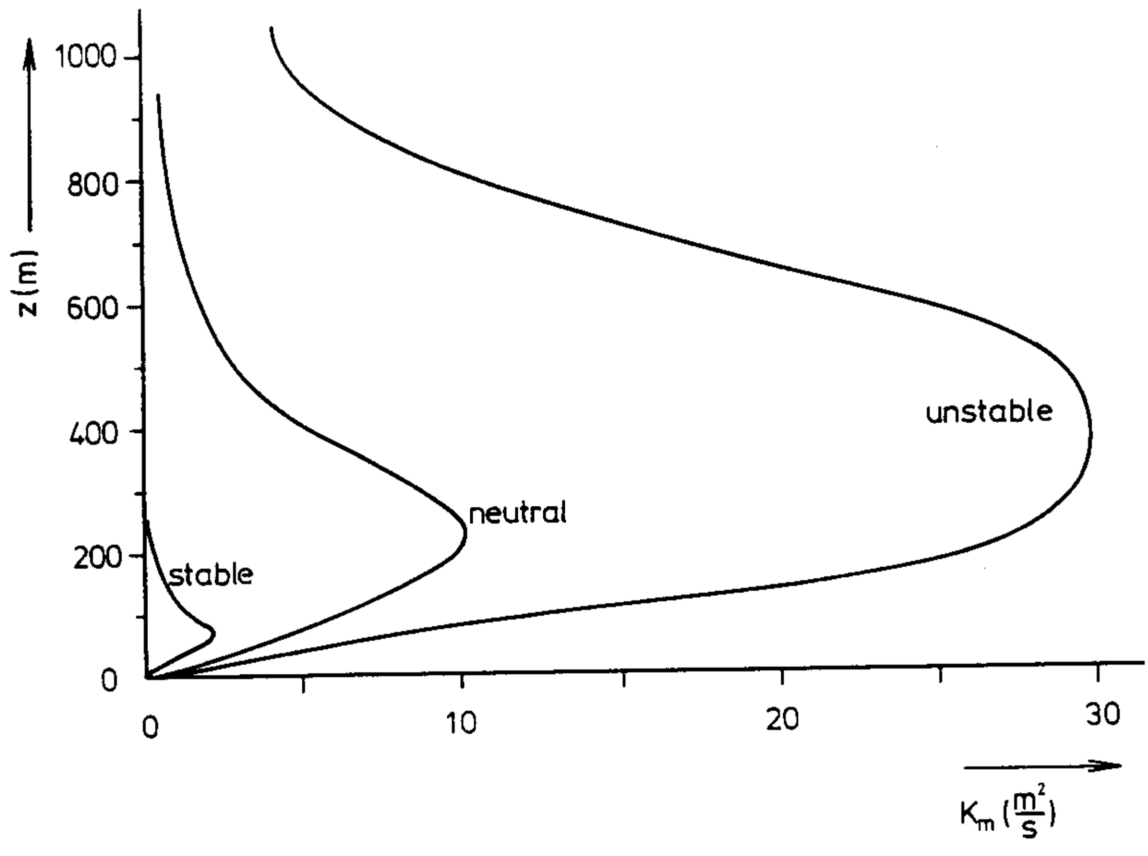

Fig. 6: Typical vertical profiles of the eddy viscosity K_m.

hypothesis" has been applied quite often in atmospheric modelling. In general form, the eddy viscosity is assumed to be related to the deformation for the mean velocity field by:

$$K_m = \ell^2 \left| \frac{\partial \overline{u_i}}{\partial x_k} + \frac{\partial \overline{u_k}}{\partial x_i} \right| \tag{33}$$

Here ℓ is called "mixing length" and is a representative measure of the scale of the turbulent eddies in the flow under consideration, hence ℓ is also termed "turbulent length scale". In the atmospheric boundary layer, where vertical gradients are usually predominant, (33) may be written in the more familiar way:

$$K_m = \ell^2 \left| \frac{\partial \overline{u_i}}{\partial z} \right| \tag{34}$$

where $\overline{u_i}$ denotes the horizontal wind velocity vector.

In order to apply (34) to real flow situations the mixing length ℓ has be to described in order to close the set of equations. This has led to numerous proposals in the literature which can not be treated here extensively. For more details we refer to papers by Wippermann (1973), Clarke (1974), Yu (1977), Mc Bean (1979) or Bodin (1980) where a collection of different mixing length formulations can be found.

Instead as an example the widely used mixing length profile due to Blackadar (1962) is given, which reads:

$$\ell(z) = \frac{\kappa z}{1 + \frac{\kappa z}{\lambda}} \tag{35}$$

Here λ is the assymptotic value of the mixing length ℓ for large z, i.e. in the upper part of the atmospheric boundary layer. λ may be related to the geostrophic wind v_g by

$$\lambda = 2.7 \ 10^{-4} \frac{|v_g|}{f} \tag{36a}$$

or to the friction velocity u_* by

$$\lambda = 6.3 \ 10^{-3} \frac{u_*}{f} \tag{36b}$$

where f is the Coriolis parameter.

The proposed mixing length profile (33) has a linear increase near the surface (like in the surface layer, see Chap. 3) and approaches the limiting value $\ell = \lambda$ (typically 30 m) in the upper part of the boundary layer.

As an example simulations of the so-called Leipzig wind profile (Lettau, 1950) with mixing length profile (35) are shown in Fig. 7 - 9 (after Detering, and Etling, 1985). In this case the observed geostrophic wind was V_g = 17.5 m/s and the roughness length z_0 =0.3 m. The lowest layer with $z_0 < z < z_s$ was modelled using the logarithmic wind profile (Eq. 19), where z_s is the height of the surface layer and also the lowest computational grid point. The mixing length formulation seems to agree reasonable with observations, but this is expected as this profile has been fitted, among others, to the measurements of Leipzig wind profile. Although this case is just an example of wind profiles observed in the ABL, simulations in Fig. 7 - 9 give an impression of the typical vertical variation of mixing length ℓ and eddy viscosity K_m, as well as for the horizontal wind components $\overline{u}$ and $\overline{v}$, in the neutral atmospheric boundary layer for strong geostrophic winds.

4.4 Influence of Thermal Stratification on the Mixing Length

As already stated in Chap. 4.2, the magnitude of the turbulent diffusivities (or exchange coefficients) depends also on the thermal stability of the atmosphere. If we apply this idea to the mixing length approximation (33), (34), the influeance of stratification should be incorporated into the formulation of the mixing length ℓ (z). Many modifications of the neutral mixing length, denoted by ℓ_n in the following, by stratification have been proposed by various authors (see Wippermann 1973), Clarke (1974), Yu (1977), Mc Bean (1979), Therry and Lacarrère (1983), Detering (1985), Lacser and Arya (1986) for collections of proposed formulations. Here we

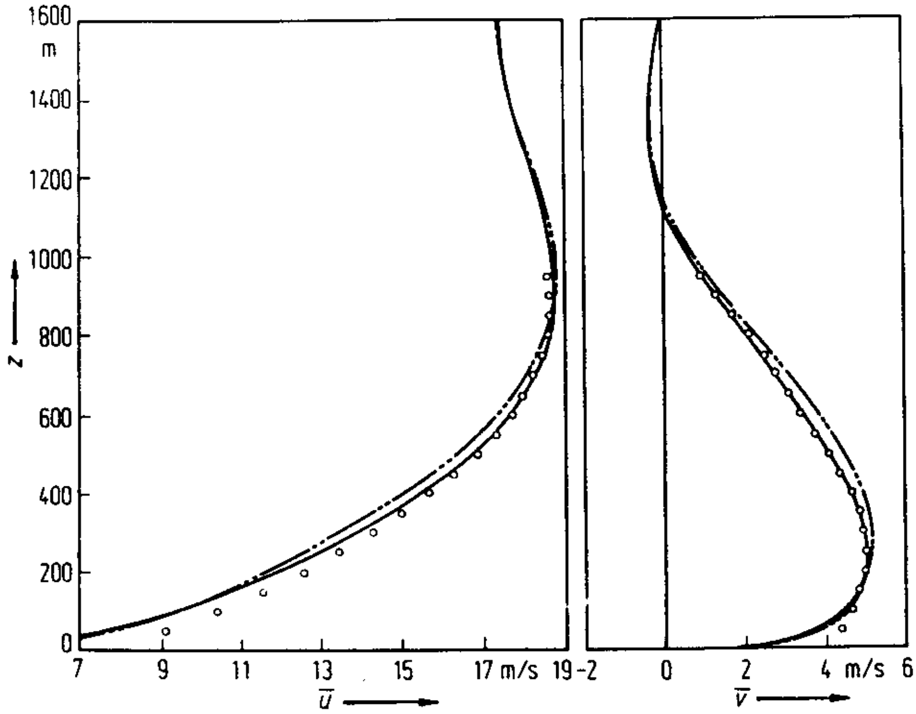

Fig. 7: Horizontal wind components $\overline{u}$ and $\overline{v}$ for the Leipzig windprofile (o o o) compared to results from a numerical model (after Detering and Etling, 1985).

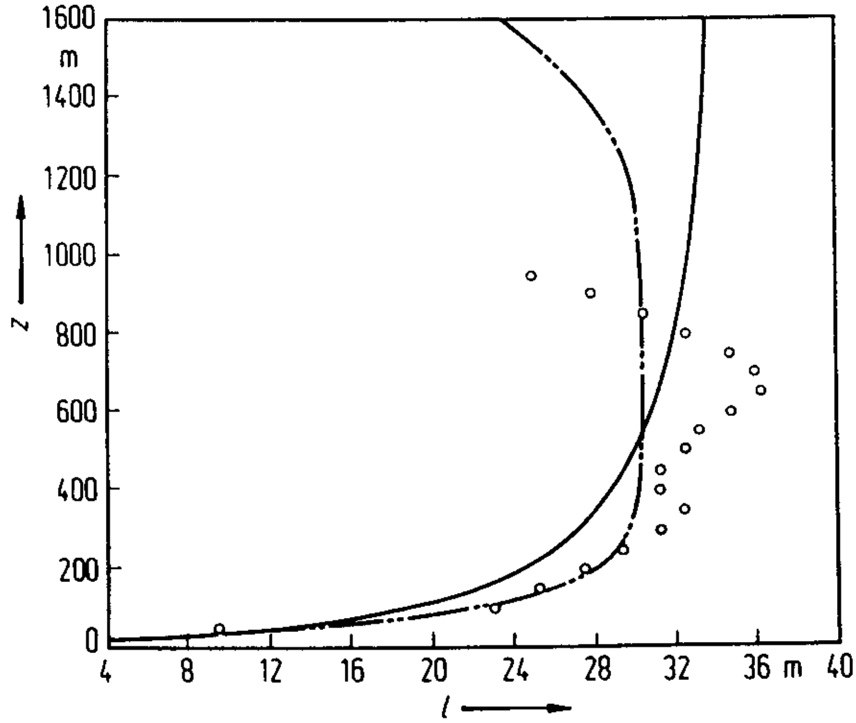

Fig. 8: Same as figure 7 but for the mixing length ℓ.

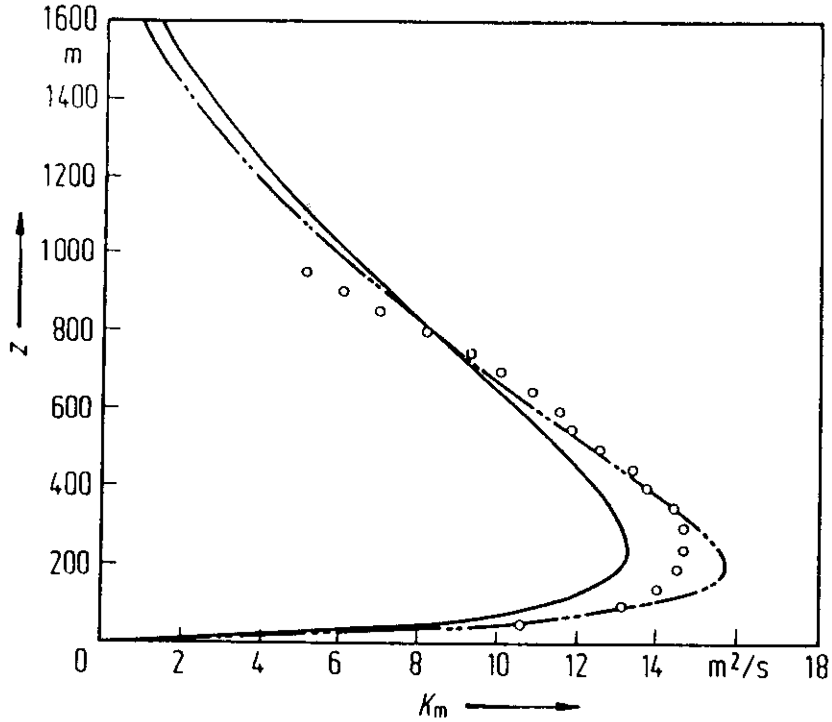

Fig. 9: Same as figure 7 but for the eddy viscosity K_m.

will give only few examples of methods incorporating the influence of stratification into the mixing length approach.

If the mixing length ℓ is regarded as a characteristic length scale of the so-called "energy-containing-eddies" in turbulent flows, the result obtained so far may be interpreted as follows: under unstable stratification the size of the turbulent eddies is enhanced by buoyancy forces, whereas the size is reduced under the action of gravity in stably stratified flows.

It is quite common to use the so-called Richardson Number Ri as a measure of stratification in the atmosphere:

$$Ri = \frac{\frac{g}{\overline{\theta}}\frac{\partial\overline{\theta}}{\partial z}}{\left(\frac{\partial\overline{u}}{\partial z}\right)^2 + \left(\frac{\partial\overline{v}}{\partial z}\right)^2} \tag{37}$$

In (37) the consideration of the vertical shear of both velocity components $\overline{u}$ and $\overline{v}$ is necessary in the atmospheric boundary layer due to the turning of the wind with height (see Fig. 5). Many relations for the modification of the mixing length by stratification expressed through the Richardson number have been proposed in the literature. A collection of different forms may be found in Blackadar (1979), from which we quote the following proposals:

(a) unstable stratification (Ri <0):

$$\ell = \ell_n(1 - 18Ri)^{1/4} \tag{38}$$

(b) stable stratification ($0 < Ri < 0.2$):

$$\ell = \ell_n(1 - 5Ri) \tag{39}$$

where ℓ_n is again the mixing length for neutral stratification.

The influence of thermal stratification on the mixing length in the ABL is shown schematically in Fig. 10.

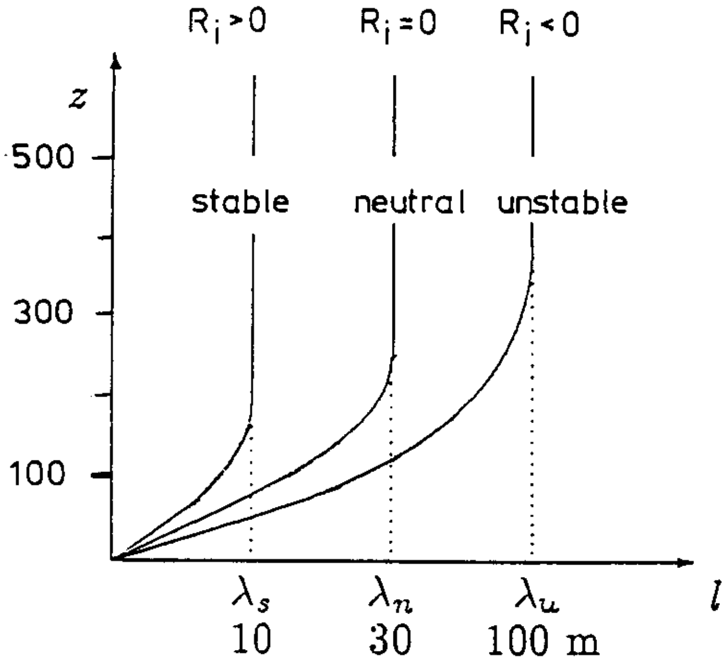

Fig. 10: Typical profiles of the mixing length ℓ for different stratification.

The form (39) used for stable stratification implies a critical Richardson number $Ri_c = 0.2$. i.e. $\ell \to 0$ for $Ri > Ri_c$, which physically means vanishing turbulence for large positive values of the Richardson number. But as the critical Richardson number is still a matter of discussion, and a vanishing mixing length also leads to $K_m = 0$ (which is not always desirable in numerical modelling), also other mixing length formulations for the stable case have been proposed. An example as given by Gutman and Torrance (1975) may be written:

$$\ell = \ell_n(1 + 3Ri)^{-1/2} \quad , \quad Ri > 0 \tag{40}$$

In this case $\ell \to = 0$ for $Ri \to \infty$ in an asymptotic way without defining a critical Richardson number a priory.

Although the relations (38) – (40) give some idea how to incorporate thermal stratification into the mixing length profiles, the correct method is still debatable as can be seen from the different papers quoted in this context.

4.5 Equation for the Turbulent Kinetic Energy

In the mixing length approach (33) or (34) the eddy viscosity K_m was related to the local deformation of the mean velocity field. But as eddy viscosity may also depend on time history and turbulence properties of the flow under consideration, a slightly different mixing length formulation has become quite popular in turbulence modelling. Here instead of the deformation tensor the turbulent kinetic energy (TKE) defined by

$$E = 0.5\overline{u_i'^2} = 0.5\,(\overline{u'^2} + \overline{v'^2} + \overline{w'^2}) \tag{41}$$

has been used for a mixing length hypothesis. This approach may be called "Prandtl-Kolmogorov" relation and is termed "level 1.5" approximation in the closure hierarchy developed by Mellor and Yamada (1974). It reads:

$$K_m = c_e\,\ell\,E^{1/2} \tag{42}$$

where ℓ is the mixing length as in (33), (34) and c_e a constant. Although there are slightly different values for c_e offered in the literature (see Detering and Etling (1985) for a collection), we may adopt the value $c_e = 0.4$ here.

Besides from the problem, that the mixing length ℓ has to be specified an additional equation for the turbulent kinetic energy E has to be used for closing the problem. This equation (see e.g. Busch (1973) or Businger (1982) for a derivation) may be written as:

$$\frac{\partial E}{\partial t} + \overline{u_i}\frac{\partial E}{\partial x_i} = P_m + P_t - \varepsilon + \frac{\partial}{\partial x_i}K_e\frac{\partial E}{\partial x_i} \tag{43}$$

In (43) P_m denotes the production of turbulent kinetic energy by mechanical forces and P_t the production (or dissipation) by buoyancy forces, described by:

$$P_m = -\overline{u_k'u_i'}\,\frac{\partial \overline{u_i}}{\partial x_k} \tag{44a}$$

$$P_t = \frac{g}{\overline{\theta}}\,\overline{w'\theta'} \tag{44b}$$

The production terms P_m and P_t in (43) may be also written with the vertical gradients of the mean variables using the boundary layer approximation as:

$$P_m = K_m\left[\left(\frac{\partial \overline{u}}{\partial z}\right)^2 + \left(\frac{\partial \overline{v}}{\partial z}\right)^2\right] \tag{45a}$$

$$P_t = -\frac{g}{\overline{\theta}}\,K_h\,\frac{\partial \overline{\theta}}{\partial z} \tag{45b}$$

The turbulent diffusivity for kinetic energy K_e in (43) is usually related to the eddy viscosity K_m by $K_e = cK_m$, where the constant c is about 1.3. Also often the relation $K_e = K_h$ is used for simplicity.

The energy-dissipation ε still has to be determined in Eq. (43). This is usually done by the so-called Kolmogorov relation

$$\varepsilon = c_\varepsilon \frac{E^{\frac{3}{2}}}{\ell} \tag{46}$$

where ℓ again is the mixing length. The constant c_ε is related to the constant c_e in Eq. (42) by $c_\varepsilon = c_e^3$ (see e.g. Detering and Etling, 1985). Hence with $c_e = 0.4$ one would get $c_\varepsilon = 0.064$.

For application of the Prandtl-Kolmogorov closure (42) and (43) to numerical modelling also boundary conditions for the turbulent kinetic energy E have to be specified. Whereas at the top of the boundary layer (z = h, or z = z_i) usually the condition $E = 0$ is applied, there is no obvious condition for the lower boundary at the earth's surface. Observations show that the turbulent kinetic energy in the surface layer is related to the friction velocity u_* by:

$$E = {u_*}^2/{c_e}^2 \quad , \quad z_0 < z < z_s \tag{47}$$

where z_s is the top of the surface layer and c_e is the same constant as used in Eq. (42). Indeed if (47) is inserted in the Prandtl-Kolmogorov relation (42) one yields $K_m = \ell u_*$ which is the same as (22a) for the eddy viscosity in the surface layer under neutral stratification.

But one has to keep in mind, that all closure methods for turbulent fluxes contain some empirical assumptions, which might not be applicable to real atmospheric flows in all situations. As an example we might mention that simple first order closure models like (11) - (13) are not suitable under very stable ($h/L > 5$) or very unstable ($h/L <$ -10) conditions for describing turbulent transport (Wyngaard, 1985). In those cases turbulent fluxes may be even up-gradient of mean quantities, implying a negative diffusivity in flux-gradient relations like (11) - (13). In order to handle these problems of buoyancy-dominated turbulence in the parameterization of turbulent fluxes, some kind of integral closure methods have been proposed recently (Fiedler and Moeng, 1985; Stull and Driedonks, 1987), but will not be discussed in this context.

4.6 Turbulent fluxes

As the flow in the ABL is usually turbulent, one might be also interested in the vertical profiles of turbulence quantities as already discussed for the surface layer in Chap. 3.1. Although data on these quantities are not easily obtained in the lowest 1000m of the atmosphere, typical profiles of the turbulent heat flux $\overline{w'\Theta'}$, momentum flux $\overline{w'u'}$, $\overline{w'v'}$ (also called Reynolds-stress) and the velocity variances $\overline{u'^2}, \overline{v'^2}, \overline{w'^2}$ have been documented through various field experiments (see data collections in the books by Nieuwstadt and van Dop, 1982, Lenschow, 1986; Arya, 1988; Stull, 1988; Garratt, 1992).

Some examples of vertical profiles of various turbulence quantities are given in Figs. 11–13. In general, turbulent heat and momentum flux as well as temperature and velocity variances are decreasing with height and vanish above the ABL height $z = h$. The maximum values can be found at the lower boundary, i.e. at $z = z_0$. This is due to the fact, that near the ground vertical gradients of mean wind and mean temperature are very large and thus give rise to strong turbulent fluxes.

Some exceptions from this behaviour can be found in the so-called convective boundary layer under unstably stratified conditions. Here some regions of negative heat flux can be observed near the top of the ABL (Fig. 11) which is due to entrainment of warm air from above the temperature inversion (see also Fig. 3). Also the velocity variances sometimes have a maximum in the middle of the ABL and not at the ground, which is related to the appearance large-scale structures (plumes and thermals) in a strongly heated boundary layer (Fig. 12).

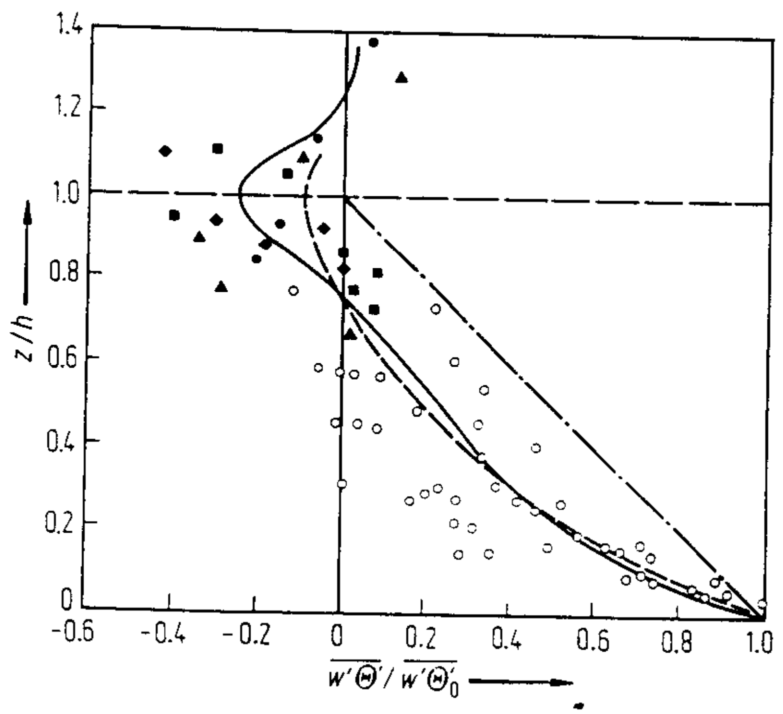

Fig. 11: Normalized turbulent heat flux as a function of normalized height z/h in the unstably stratified ABL (after Caughey, 1982).

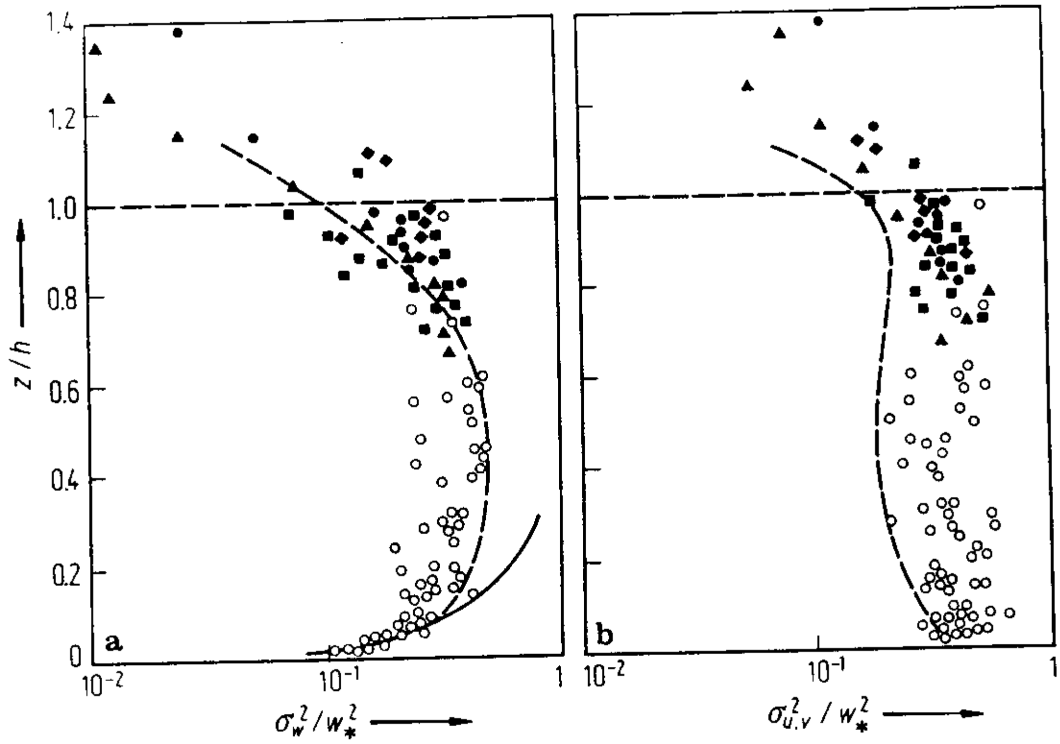

Fig. 12: Velocity variances normalized with the convective velocity scale w_* as function of z/h in the unstably stratified ABL (after Caughey, 1982).

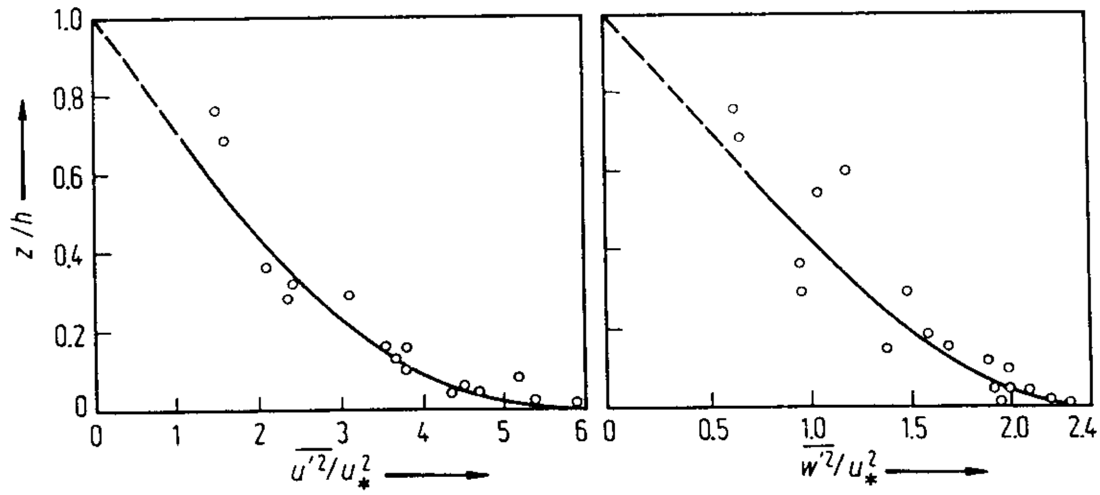

Fig. 13: Velocity variances normalized with the friction velocity u_* as function of height z/h for a stably stratified ABL (after Caughey, 1982).

5 Applications of ABL theory

This lectures on the atmospheric boundary layer might seem very specialized within the workshop on Fluid Mechanics. But if we look for practical applications we will find, that knowledge of ABL physics is essential for various fields in meteorology and engineering. In order to illustrate this, we will give some examples below.

Prediction of weather and climate

As weather we may simply define the variation of the atmosphere e.g. wind, temperature, humidity, clouds, rain within global spatial scale and temperature variation within days. Climate might be defined as the temporal variation of global weather within time-scales of months, years or decades. The prediction of weather and climate by means of numerical models is an actual task performed by hundreds of scientists worldwide. Although the ABL covers only about 1/10 of the volume of the whole atmosphere, it is also the lower boundary of the troposphere and all exchanges of physical and chemical quantities between the earth's surface (continents and oceans) and the free atmosphere are taking place at this lower boundary. Hence it is very important to know the excact transfer of momentum, heat, moisture and trace substances from the surface to the atmosphere and vice versa. For this reason, knowledge of the turbulent exchange processes in the ABL is neccessary in order to obtain the correct forcing of the free atmosphere from below. As one excample we might mention the heat exchange between the land surface and the overlying atmospheric layer which lead to the diurnal variation of air temperature in the ABL, as ist discussed in some details in Part II of this lecture. On the other hand, ocean circulations are driven to a great part by wind forces applied to the water surface, hence knowledge of the surface wind stress (e.g. $\overline{w'u'}$) is required for calculation of ocean currents. More information on the role of the ABL in weather and climate prediction can be found in the monograph "The Atmospheric Boundary Layer" (Garratt, 1992).

Air pollution problems

The pollution of the earth's atmosphere by antropogenic sources is one of the major environmental problems of our society. Except for aircraft emissions, all pollutants are produced near the earth's surface, where human life takes place. Hence it is obvious, that the ABL is the most polluted part of the whole atmosphere. And as all people are living on the earth's surface, the effects of air pollution on mankind is pronounced in the ABL.

Now what has boundary layer physics to do with this problem? All pollutants set free by industrial or natural sources are transported with the wind from their source to other regions of the near surface layer of the atmosphere. Vertical and lateral dispersion of pollutants is due to turbulent motions in this layer. This can be illustrated by means of the equation for air admixtures (Eq. 9), which is repeated here.

$$\frac{\partial \overline{c}}{\partial t} + \overline{u_i}\frac{\partial \overline{c}}{\partial x_i} = \frac{\partial}{\partial x_i} K_c \frac{\partial \overline{c}}{\partial x_i} \tag{48}$$

$\overline{c}$ is the mean concentration of an air admixture, $\overline{u_i}$ is the mean wind field and K_c is the turbulent diffusivity for an air admixture c.

Although $\overline{u_i}$ and K_c are usually varying in space and time, it is sufficient for many applications in air pollution problems, to know only the vertical profiles of the wind $\overline{u}(z), \overline{v}(z)$ and of the diffusivity $K_c(z)$ (usually related to the eddy viscosity $K_m(z)$). These can be obtained from ABL theory or observations, as described in Chap. 3–4. More details on air pollution problems as related to the ABL can be found e.g. in the monograph "Atmospheric Diffusion" (Pasquill and Smith, 1983).

Wind Engineering

Under wind engineering we might summarize the applications of wind to technical problems, e.g. wind forces on buildings and structures. Also the problem of wind energy, i.e. the production of electrical power by wind converter, can be taken as an example. For the latter we know, that the power output from wind energy devices is proportional to the third power of the wind speed. Hence a good knowledge of the vertical wind profile in the lowest 100m or so above ground is very important for the proper placement of wind energy devices.

Another application of boundary layer meteorology is related to aviation safety during take-off and landing. Here strong wind shear near the ground or unexpected turbulent gusts can be hazardous to aircrafts in this situations. Most information on wind engineering problems can be found in the book "Engineering Meteorology" (Plate, 1982).

6 References

André, J.C. , Planetary boundary layer parameterization and turbulence closure, in: Mesoscale Meteorology, Theories, Observations and models, (Lilly, D.K., Gal. Chen, T. (eds.)), D. Reidel, Dordrecht 651–670 (1983).

André, J.C., De Moor, G., Lacarrère, P., Therry, G., du Vachat, R. , Modeling the 24-Hour evolution of the mean and turbulent structures of the planetary boundary layer. J.
Atmos. Sci. 35, 1861–1883 (1978).

Arya, S.P.S. , Introduction to Micrometeorology. Academic Press, (1988).

Beljaars, A.C.M., Walmsley, J.L., Taylor, P.A. , Modelling of Turbulence over low Hills and varying Surface Roughness. Boundary Layer Meteorol. 41, 203–215 (1987).

Blackadar, A.K. , The vertical distribution of wind and turbulence exchange in a neutral atmosphere. J. Geophys. Res. 67, 3095–3102 (1962).

Blackadar, A.K. , High resolution models of the planetary boundary layer. In: Advances in Environmental Science and Engineering Vol. I, Gordon and Breach, 50–63 (1979).

Bodin, S. , Applied numerical modelling of the atmospheric boundary layer, in: Atmospheric Boundary Layer Physics (Longhetto, A. ed.) Elsevier, Amsterdam, 1–76 (1980).

Bradshaw, P., Cebici, T., Whitelaw, J.H. , Engineering calculation methods for turbulent flow. Academic Press, London (1981).

Brost, R., Wyngaard, J.C. , A model study of the stably stratified planetary boundary layer. J. Atmos. Sci. 35, 1427–1440 (1978).

Brown, R.A. ,Planetary Boundary Layer Modelling. Adam Hilger, London (1974).

Brutsaert, W. , Evaporation into the Atmosphere, D. Reidel, Dordrecht (1982).

Busch, N.E. , On the mechanics of atmospheric turbulence, in: Workshop on Micrometeorology (Haugen, D.A., ed.), American Meteor. Soc., Boston, 1–66 (1973).

Busch, N.E., Chang, S.W., Anthes, R.A. , A Multi-Level Model of the Planetary Boundary Layer Suitable for Use with Mesoscale Dynamic Models. J. Appl. Meteor. 15, 909–919 (1976).

Businger, J.A. , Equations and concepts, in: Atmospheric Turbulence and Air Pollution Modelling (Nieuwstadt, F.T.M., van Dop, H. eds.) D. Reidel, Dordrecht, 1–36 (1982).

Businger, J.A., Wyngaard, J.C. Jzumi, Y, Bradley, E.F. , Flux-profile relationships in the atmospheric surface layer. J. Atmos. Sci. 28, 181–189 (1971).

Caughey, S.J. , Observed characteristics of the atmospheric boundary layer: In: Atmospheric turbulence and air pollution modelling (Nieuwstadt and van Dop, Eds.). D. Reidel, Dordrecht, 107–158 (1982).

Clarke, R.H. , Attempts to simulate the diurnal course of meteorological variables in the boundary layers. Isv. Atmos. Ocean. Phys. 10, 360–373 (1974).

Deardorff, J.W. , Three dimensional modelling of the planetary boundary layer, in: Workshop on Micrometeorology, (Haugen, D.E., ed.), Amer. Meteor. Soc., Boston, 271–312 (1973).

Deardorff, J.W. , Three-dimensional study of the height and mean structure of a heated planetary boundary layer. Boundary-Layer Meteorol. 7, 81–106 (1974).

Deardorff, J.W. , Sub-grid-scale turbulence modeling. Adv. Geophys. 28, 337–343 (1985).

Detering, H.W. , Mischungsweg und turbulenter Diffusionskoefizient in atmosphärischen Simulationsmodellen. Ber. Inst. Meteorol. und Klimatol. Univ. Hannover 25 (1985).

Detering, H.W., Etling, D. , Application of the E-ε-turbulence model to the atmospheric boundary layer. Boundary-Layer Meteorol. 33, 113–133 (1985).

Dyer, A.J. , A review of flux-profile relationships. Boundary-Layer Meteorol. 7, 363–372 (1974).

Ekman, V.W. , On the influence of earth's rotation on ocean currents. Ark. Month. Astron. O. Fysik. 2, 11–21, 1905.

Etling, D. , The planetary boundary layer. In: Landolt-Börnstein New Series, V4/c1: Meteorology, Springer, Berlin, 151-188 (1987).

Etling, D., Detering, H.W., Wamser, M. , Parameterisierung turbulenter Flüsse in mesoskaligen Simulationsmodellen: Eine Fallstudie mit Schließungsansätzen erster Ordnung. Meteorol. Rdsch. 39, 178–188 (1986).

Fiedler, B.H., Moeng, C.H. , A practical integral closure model for mean vertical transport of a scalar in a convective boundary layer. J. Atmos. Sci. 42, 359–363 (1985).

Groß, G. , Some effects of defore station on nocturnal drainage flow and local climate - a numerical study. Boundary-Layer Meteorol. 38, 315–337 (1986).

Garratt, I.R. , The Atmospheric Boundary Layer. Cambridge University Press, 1992.

Gutman, D.P., Torrance, K.E. , Response of the urban boundary layer to heat addition and surface roughness. Boundary-Layer Meteorol. 9, 217–233 (1975).

Hinze, J.O. , Turbulence. Mc Graw-Hill, New York (1975, second Edition).

Kitada, T. , Turbulence structure of sea breeze front and its implication in air pollution transport – Application of the K-ε turbulence model. Boundary-Layer Meteorol. 41, 217–239 (1987).

Lacser, A., Arya, S.P.S. , A comparative assessment of mixing-length parameterizations in the stably stratified nocturnal boundary layer (NBL). Boundary-Layer Meteorol. 36, 53–70 (1986).

Launder, B.E., Spalding, D.B. , Mathematical models of turbulence. Academic Press, London (1972).

Lenschow, D.H. , Probing the Atmospheric Boundary Layer. Amer. Meteorol. Soc., Boston (1986).

Lesieur, M. , Turbulence in Fluids. Martinus Nijhoff, Dordrecht (1987).

Lettau, H. , A re-examination of the "Leipzig Wind Profile" considering some relations between wind and turbulence in the fridional layer. Tellus 2, 125–129 (1950).

Louis, J.F. , A parametric model of vertical eddy fluxes in the atmosphere. Boundary-Layer Meteorol. 17, 187–202 (1979).

Louis, J.F., Tiedtke, M., Geleyn, J.F. , A short history of the PBL parameterization at ECMWF. In: Workshop on planetary boundary layer parameterization (ECMWF, Reading), 59–80 (1981).

Lumley, J.L., Khajeh-Nouri, B. , Computational modelling of turbulent transport, in: Advances in Geophysics, Vol. 18a, Academic Press, New York, 169–192 (1974).

Mason, P.J., Callen, N.S. , On the magnitude of the subgridscale eddy coefficient in large-eddy simulations of turbulent channel flow. J. Fluid Mech. 162, 439–462 (1986).

Mason, P.J., Thomson, D.J. , Large-eddy simulations of the neutral-static-stability planetary boundary layer. Quart. J.R. Met. Soc. 113, 413–443 (1987).

Mc Bean, G.A. (ed.) , The Planetary Boundary Layer, WMO TN 165, WMO, Geneva (1979).

Mellor, G.L. , Ensemble average, turbulence closure. Adv. Geophys. 28, 345–358 (1985).

Mellor, G.L., Yamada, T. , A hierarchy of turbulence closure models for planetary boundary layers. J. Atmos. Sci. 31, 1791–1806 (1974).

Moeng, C.H. , A large-eddy-simulation model for the study of planetary boundary-layer turbulence. J. Atmos. Sci. 41, 2052–2062 (1984).

Moeng, C.H., Wyngaard, J.C. , Statistics of conservative scalars in the convective boundary layer. J. Atmos. Sci., 41, 3161–3169 (1984).

Monin, A.S., Yaglom, A.M. , Statistical fluid mechanics. M.I.T. Press, Cambridge, Vol. I (1971) Vol. II (1975).

Monin, A.S., Obukhov, A.M. , Basic laws of turbulent mixing in the atmosphere near the ground. Trudy Geofiz. Inst. Nauk. S.S.S.R. 24, 163 (1954).

Nieuwstadt, F.T.M., van Dop, H. (ed.) , Atmospheric Turbulence and Air Pollution Modelling, D. Reidel, Dordrecht (1982).

Oke, T.R. , Boundary Layer Climates, Methuen, London (1978).

Panchev, S. , Dynamic Meteorology. D. Reidel, Dordrecht (1985).

Panofsky, H.A., Dutton, J.A. , Atmospheric Turbulence, John Wiley, New York, (1984).

Pasquill, F.B., Smith, F.B. , Atmospheric Diffusion. Ellis Horwood, Chichester (1983).

Paulson, C.A. , The mathematical representation of wind speed and temperature profiles in the unstable atmospheric surface layer. J. Appl. Meteorol. 9, 857–861 (1970).

Pielke, R.A: , Mesoscale Meteorological Modellling. Academic Press, New York (1984).

Plate, E.J. , Engineering Meteorology. Elsevier, Amsterdam (1982).

Pruitt, W.O. Morgan, D.L., Laurence, F.J. , Momentum and mass transfer in the surface boundary layer. Quart. J. R. Met. Soc. 99, 370–386 (1973).

Raithby, G.D., Stubley, G.D., Taylor, P.A. , The Askervein hill project: A finite control volume prediction of three-dimensional flows over the hills. Boundary-Layer Meteorol. 39, 247–267 (1987).

Rodi, W. , Turbulence models for environmental problems. In: Prediction methods for turbulent flows (W. Kollman Edit.), Hemisphere Publ. Corp., Washington, 259–350 (1980).

Rodi, W. , Calculations of stably stratified shear flows with a buoyancy-extended k-ε turbulence model. In: Turbulence and diffusion in stable environments (Hunt, J.C.R., ed.), Oxford University Press, Oxford, 111–140 (1985).

Schumann, U. , Subgrid scale model for finite-difference simulations of turbulent flows in plane channels and annuli. J. Comp. Phys. 18, 376–404 (1975).

Schumann, U., Friedrich, R. , Direct and large eddy simulation of turbulent flows. Vieweg Verl., Braunschweig (1986).

Sheu, P.J., Agee, E.M., Tribbia, J.J. , A numerical study of physical processes affecting convective cellular geometry. J. Met. Soc. Japan. 58, 489–498 (1980).

Sommeria, G. , Numerical modeling of the planetary boundary layer, in: Mesoscale Meteorology, Theories, Observations and Models, (Lilly, D.K., Gal-Chen, T. (eds.)), D. Reidel, Dordrecht, 681–704 (1983).

Stull, R.B. , An Introduction to Boundary Layer Meteorology. Kluwer Academic Publishers, Dordrecht (1988).

Stull, R.B., Driedonks, A.G.M. , Applications of the transilient turbulence parameterization to atmospheric boundary-layer simulations. Boundary-Layer Meteor. 40, 209–239 (1987).

Tennekes, H., Lumley, J.L. , A first course in turbulence. MIT Press, Cambridge (1972).

Therry, G., Lacarrère, P. , Improving the eddy kinetic energy model for planetary boundary layer description. Boundary-Layer Meteorol. 25, 63–88 (1983).

Wichmann, M., Schaller, E. , On the determination of the closure parameters in higher-order closure models. Boundary-Layer Meteorol. 37, 323–341 (1986).

Williams, G.P. , Friction term formulation and convective instability in a shallow atmosphere. J. Atmos. Sci. 29, 870–876 (1972).

Wippermann, F. , The Planetary Boundary Layer, Deutscher Wetterdienst, Offenbach (1973).

Wittich, K.P., Roth, R. , A case study of nocturnal wind and temperature profiles over the inhomogneous terrain of northern Germany with some considerations of turbulent fluxes. Boundary-Layer Meteorol. 28, 169–186 (1984).

Wyngaard, J.C. , Boundary layer modelling, in: Atmospheric Turbulence and Air Pollution Modelling (Nieuwstadt, F.T.M., van Dop, H. eds.) E. Reidel, Dordrecht, 69–106 (1982).

Wyngaard, J.C. , Structure of the planetary boundary-layer and implications for its modeling. J. Clim. Appl. Meteorol. 24, 1131–1142 (1985).

Wyngaard, J.C., Coté, O.R., Rao, K.S. , Modelling the atmospheric boundary layer, in: Advances in Geophysics, Vol. 18A, Academic Press, New York, 193–212 (1974).

Wyngaard, J.C., Brost, R.A. , Top-down and bottom-up diffusion of a scalar in the convective boundary layer. J. Atmos. Sci. 41, 1959–1969 (1984).

Yaglom, A.M. , Comments on wind and temperature fluxprofile relationships. Boundary-Layer Meteorol. 11, 89–102 (1977).

Yamada, T. , Siumulations of nocturnal drainage flows by a $q^2\ell$ turbulence closure model. J. Atmos. Sci. 40, 91–106 (1983).

Yu, T.W. , A comparative study on parameterization of vertical turbulent exchange processes. Mon. Wea. Rev. 105, 57–66 (1977).

Zeman, O. , Progress in the modeling of planetary boundary-layers. A review. Ann. Rev. Fluid. Mech. 13, 253–272 (1981).

Appendix 1-D Boundary Layer Model

For computer demonstrations we choose a simple 1-D model for neutrally stratified boundary layer.

The model equations read:

$$\frac{\partial u}{\partial t} - fv = \frac{\partial}{\partial z} K_m \frac{\partial u}{\partial z} \quad \text{(A1)}$$

$$\frac{\partial v}{\partial t} + f(u - u_g) = \frac{\partial}{\partial z} K_m \frac{\partial v}{\partial z} \quad \text{(A2)}$$

In A1, A2 the x-axis (u-component) is aligned with the geostrophic wind u_g.

Boundary conditions:

$$\text{bottom} : z = z_0 : u = v = 0 \quad \text{(A3)}$$

$$\text{top} : z = h : u = u_g, v = 0 \quad \text{(A4)}$$

Solution of eq. (A1, A2) as combination of surface layer laws (chapter 3.2) and mixing length approach (chapter 4.3) for the Ekman layer:

(a) surface layer : $z_0 \leq z \leq z_s$

$$K_m = \kappa u_* z \quad \text{(A5)}$$

$$\overline{u}(z) = \frac{u_*}{\kappa} \ln\left(\frac{z}{z_0}\right) \cos\alpha_0 \quad \text{(A6)}$$

$$\overline{v}(z) = \frac{u_*}{\kappa} \ln\left(\frac{z}{z_0}\right) \sin\alpha_0 \quad \text{(A7)}$$

α_0 is the angle between the wind vector $\vec{v}_s$ at $z = z_s$ and the geostrophic wind u_g (cross-isobar-angle). z_s is taken as $z_s = 25$ m.

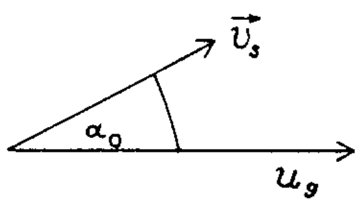

(b) Ekman layer: $z_s \leq z \leq h$

$$K_m = l^2 \left[\left(\frac{\partial u}{\partial z}\right)^2 + \left(\frac{\partial v}{\partial z}\right)^2\right]^{1/2} \quad \text{(A8)}$$

$$\text{with} \quad l = \frac{\kappa z}{1 + \frac{\kappa z}{\lambda}} \quad \text{(A9)}$$

$$\text{and} \quad \lambda = 2.7 \; 10^{-4} u_g / f \quad \text{(A10)}$$

Wind components $u(z), v(z)$ obtained as steady state solution from (A1, A2) by numerical integration.

Friction velocity u_* and angle α_0 needed in (A5 - A7) are obtained by iteration in combination with (A1, A2).

Model input: geostrophic wind u_g and roughness length z_0
Model output: $u_*, \alpha_0, u(z), v(z), K_m(z)$

Example: $u_g = 10$ m/s, $z_0 = 1$ m $\rightarrow u_* = 0.41$ m/s, $\alpha_0 = 29.6°$

Profiles of wind velocity components for this case are shown in Fig. A2 and as a wind-hodograph in A1. Eddy viscosity K_m is shown in Fig. A3.

For steady state ($\partial/\partial t = 0$) an analytical solution for A1, A2 can be found using a two layer model:

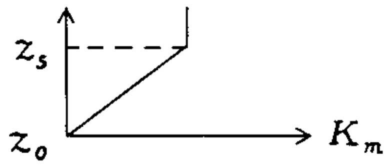

Ekman layer: $K_m = \kappa u_* z_s, \quad z > z_s$
Surface layer: $K_m = \kappa u_* z, \quad z_0 \leq z \leq z_s$

Windprofiles (analytical solution):

(a) surface layer: $(z_0 \leq z \leq z_s)$

$$\overline{u}(z) = \frac{u_*}{\kappa} ln \left(\frac{z}{z_0}\right) \cos\alpha_0 \qquad \text{(A11)}$$

$$\overline{v}(z) = \frac{u_*}{\kappa} ln \left(\frac{z}{z_0}\right) \sin\alpha_0 \qquad \text{(A12)}$$

(b) Ekman layer $(z > z_s)$

$$\overline{u}(z) = u_g \left(1 - \sqrt{2} \exp\left(-\frac{z - z_s}{D}\right) \sin\alpha_0 \cos\left(\frac{z - z_s}{D} + \frac{\pi}{4} - \alpha_0\right)\right) \qquad \text{(A13)}$$

$$\overline{v}(z) = u_g \left(\sqrt{2} \exp\left(-\frac{z - z_s}{D}\right) \sin\alpha_0 \sin\left(\frac{z - z_s}{D} + \frac{\pi}{4} - \alpha_0\right)\right) \qquad \text{(A14)}$$

$$\text{with} \quad D = (2\kappa u_* z_s / f)^{1/2} \qquad \text{(A15)}$$

α_0 is the cross-isobar angle as defined above.

Model input: geostrophic wind u_g
roughness length z_0
surface layer height z_s

Model output: u_*, α_0 obtained by matching solutions (A11,A12)
with (A13, A14) at $z = z_s$ by iteration
u(z), v(z) with u_*, α_0 from A11 - A14

The variation of the surface layer height z_s may be regarded as influence of thermal stratification. Typical values may be:

$z_s = 10$ m stable stratification
$z_s = 30$ m neutral stratification
$z_s = 50$ m unstable stratification

Typical range of friction velocity u_* : 0.1 - 0.5 m/s
Typical range of cross-isobar angle α_0 : 10° - 40°

Typical variation of u_* (and also of $K_m = \kappa u_* z_s$) and α_0 with the input parameters u_g, z_0 and z_s are shown below.

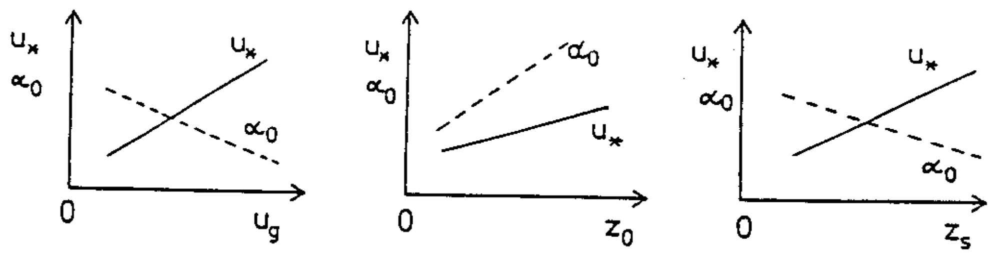

The analytical model A11 - A14 is also used as initial profile for starting the numerical solution of boundary layer model A1 - A10. Both can be run interactively at the PC's.

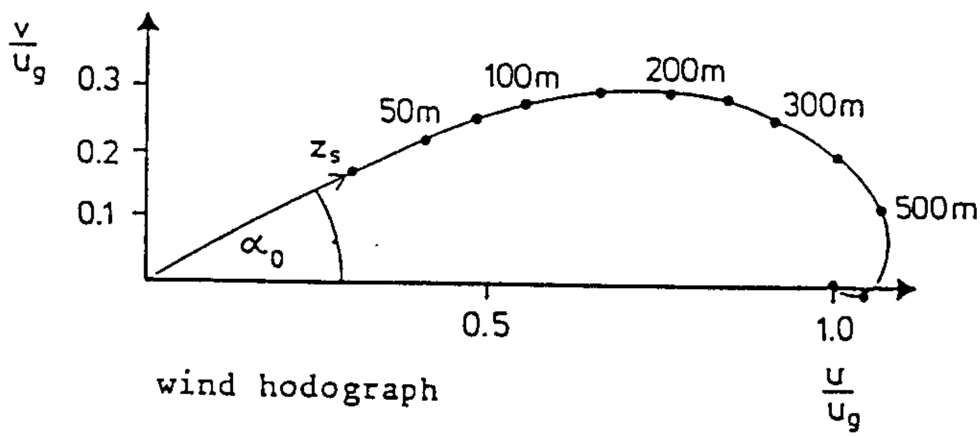

Fig. A1: Wind hodograph (Ekman-spiral) resulting from a boundary layer model with $u_g = 10$ m/s^{-1} and $z_0 = 1$ m.

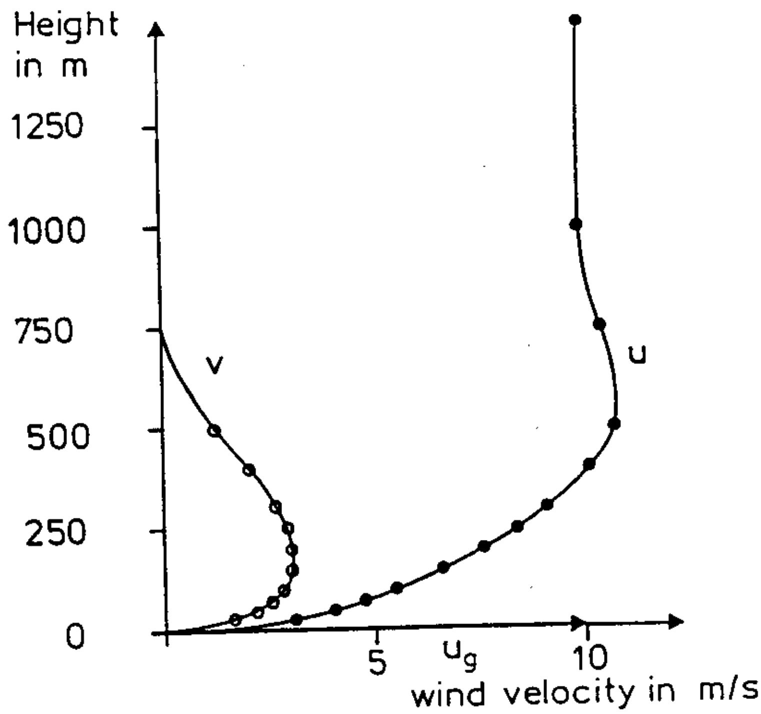

Fig. A2: Same as Figure A1 but for the wind profiles $u(z)$ and $v(z)$.

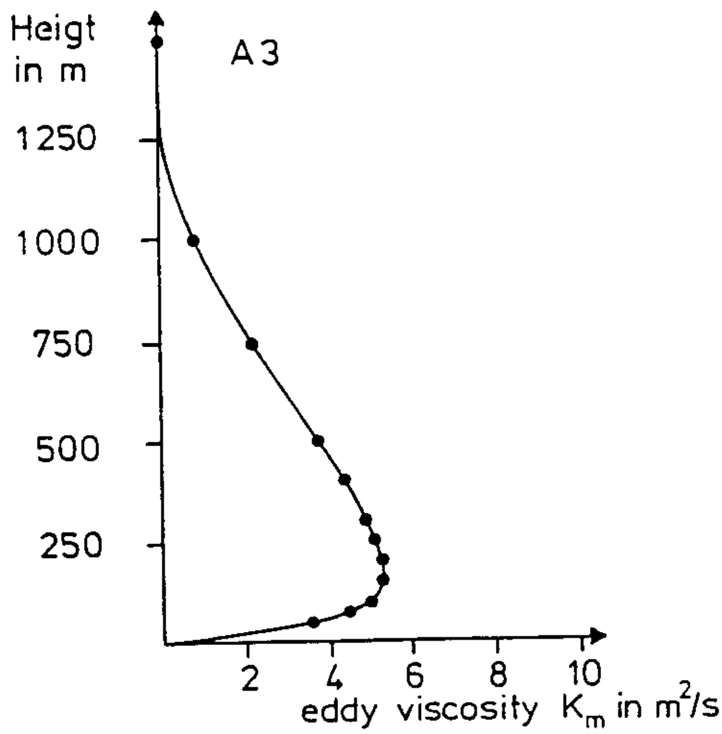

Fig. A3: Same as Figure A1 but for the eddy viscosity $K_m(z)$.